

On the recent warming of the southeastern Bering Sea shelf

P.J. Stabeno*, N.A. Bond, S.A. Salo

NOAA/Pacific Marine Environmental Laboratory, 7600 Sand Point Way NE, Seattle, WA 98115-6349, USA

Received in revised form 25 January 2007; accepted 2 August 2007

Available online 19 November 2007

Abstract

During the last decade, the southeastern Bering Sea shelf has undergone a warming of $\sim 3^\circ\text{C}$ that is closely associated with a marked decrease of sea ice over the area. This shift in the physical environment of the shelf can be attributed to a combination of mechanisms, including the presence over the eastern Bering Sea shelf of a relatively mild air mass during the winter, especially from 2000 to 2005; a shorter ice season caused by a later fall transition and/or an earlier spring transition; increased flow through Unimak Pass during winter, which introduces warm Gulf of Alaska water onto the southeastern shelf; and the feedback mechanism whereby warmer ocean temperatures during the summer delay the southward advection of sea ice during winter. While the relative importance of these four mechanisms is difficult to quantify, it is evident that for sea ice to form, cold arctic winds must cool the water column. Sea ice is then formed in the polynyas during periods of cold north winds, and this ice is advected southward over the eastern shelf. The other three mechanisms can modify ice formation and melt, and hence its extent. In combination, these four mechanisms have served to temporally and spatially limit ice during the 5-year period (2001–2005). Warming of the eastern Bering Sea shelf could have profound influences on the ecosystem of the Bering Sea—from modification of the timing of the spring phytoplankton bloom to the northward advance of subarctic species and the northward retreat of arctic species. Published by Elsevier Ltd.

Keywords: Bering Sea; Circulation; Climate; North Pacific; Physical oceanography; Sea ice

Regional index terms: Southeastern Bering Sea shelf; Decadal variability; Heat content; Seasonal Sea ice; Mean currents

1. Introduction

The 500-km-wide continental shelf of the eastern Bering Sea supports some of the United States' most productive and valuable fisheries, and immense populations of marine birds and mammals that contribute to the subsistence of communities of Native American peoples. It is a major economic, social, and environmental resource for the United States. Like all high-latitude ecosystems, the Bering

Sea is sensitive to shifts in climate on temporal scales ranging from interannual (e.g., El Niño/Southern Oscillation (ENSO)) through decadal (e.g., Pacific Decadal Oscillation (PDO) and the Arctic Oscillation (AO)) to long-term secular trends. In fact, although the Bering Sea is dominated by year-to-year variability, dramatic shifts in the physical, and biological environment of the southeastern Bering Sea have occurred recently (e.g., Stabeno and Overland, 2001; Overland and Stabeno, 2004; Overland and Wang, 2005a, b). It is an open question whether these changes are due more

*Corresponding author. Tel.: +1 206 526 6453.

to regional effects or to fluctuations in hemispheric modes of variability.

Sea-ice cover, a defining characteristic of any arctic or subarctic system, is decreasing in duration and concentration over the southeastern Bering Sea shelf (Overland and Stabeno, 2004), and is characterized by a faster melt back in spring over the northern shelf (Grebmeier et al., 2006). There are multiple possible causes for this decrease related to changes in atmospheric forcing and oceanic conditions. Changes in the timing and spatial extent of sea-ice impact the temperature of the Bering Sea shelf and, in particular, the extent of the cold pool (the region where bottom temperatures are $<2^{\circ}\text{C}$ during the summer) over the middle shelf. They also affect the timing of the spring-phytoplankton bloom (Stabeno and Hunt, 2002; Hunt et al., 2002).

Such changes in the physical environment are capable of reorganizing the ecosystem (Hunt et al., 2002; Hunt and Stabeno, 2002), and there is evidence that this ecosystem is changing. For instance, certain cold-water species such as Greenland turbot (*Reinhardtius hippoglossoides*) and certain amphipods are no longer found in great numbers in the southern Bering Sea (Boldt, 2004). The biomass of jellyfish (medusae) rose markedly in the 1990s (Brodeur et al., 1999) and then declined rapidly beginning about 2001, with probable linkages to regional climate variations. The central feeding location of the gray whale (*Eschrichtius robustus*) has shifted from the northern Bering Sea to the Chukchi Sea (Moore et al., 2003). At the same time, there has been a decline in the productivity and overall benthic standing stock over the northern Bering Sea (Grebmeier et al., 2006). These changes have occurred at the same time as the warming of the shelf and the decrease in sea-ice cover.

Oceanographic observations in the Bering Sea have been limited by its remoteness, its size and the harsh weather that dominates this area, especially in the winter. To increase the year-round observations over the southeastern Bering Sea shelf, we established three biophysical mooring sites in 1995. Two of the sites were only occupied for a few years, but Site 2 (M2) has been occupied nearly continuously since 1995. The location of M2 was selected as an area where sea ice occurred virtually every winter for at least a short period (Stabeno et al., 1998). In 1996, a biophysical mooring was deployed farther to the northwest in a region of the middle shelf that appeared to have a weak cross-shelf flow. In 1999,

we selected this location (M4) as a second monitoring site. Data from both these sites have provided critical quantification of the changing physical environment over the southeastern Bering Sea shelf.

In this article, we first present information about the changing extent and duration of sea ice over the southeastern shelf. Next, we relate these changes to data on temperature, currents and fluorescence collected at several mooring sites on the southeastern Bering Sea shelf. Finally, we discuss four possible mechanisms that likely contributed to the observed warming over the Bering during the last decade.

2. Methods and data

Presently, both M2 and M4 are recovered and redeployed in April/May and again in September/October. When shiptime is available and ice cover permits, the mooring sites also are visited during the winter, and the moorings are recovered and redeployed then. Biophysical data, collected by instruments on the moorings, include temperature, salinity, nutrients (since 2002 at M2, and since 2003 at M4), fluorescence and currents. Each year since 1995, an upward-looking, bottom-mounted acoustic Doppler current profiler has been deployed next to the main mooring at M2, and since 2004 at M4. Before 2004 current meters (RCM-7 or RCM-9) were deployed at M4 at 2–3 depths on the main mooring. During summer, the mooring at M2 includes a surface toroid and a full suite of meteorological variables is measured in addition to oceanographic ones.

In addition to the major mooring sites of M2 and M4, simpler moorings have been deployed near the Alaska Peninsula with a goal to better understand bottom temperature and its impact on crab populations. Two moorings (C1 and C2, Fig. 1) measured temperature only near the bottom. In addition, a mooring site has been maintained for 10 years in Pavlof Bay (P1) on the south side of the Alaska Peninsula at which temperature is measured at three of these depths (20, 60, and 100 m). Moorings at all three sites are recovered and redeployed once year, usually in April or May.

Because of the presence of sea ice and the heavy fishing pressure in the region, the main mooring at each site is constructed of chain. The main mooring at M2 was moved by ice in 1995 and again in 1999, and was caught by fishing nets in 2000 and 2004. In both 1995 and 2000, the mooring was dragged

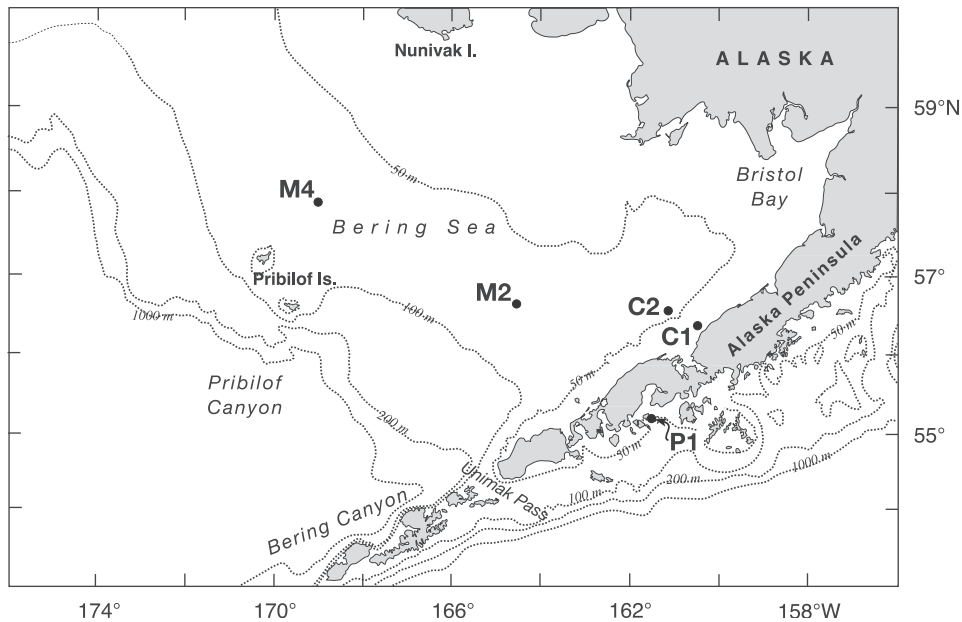


Fig. 1. Location map of the southeastern Bering Sea shelf showing the 50, 100, 200, and 1000 m isobaths. The locations of the five mooring sites discussed in the manuscript are shown.

~10 km. The other two incidents shifted the mooring by <1 km. In 1995, all equipment on the surface toroid was lost, while in the winter of 2000, the upper 20 m of the subsurface winter mooring were lost. In the other years, the mooring was recovered intact. In 1998, the release failed at M2, resulting in the mooring drifting away. It took approximately a month to deploy a replacement at M2. In contrast, M4 has been recovered intact each year.

The number and locations of instruments at M2 have evolved with time (Table 1). There are more instruments on the mooring during the summer than during the winter, when the water column is usually well mixed and there is less biological activity. The upper instrument on the subsurface moorings (both deployments at M4 and the winter deployment at M2) is at 10–11 m. While this does not present a problem of undersampling in the winter, it can present a problem in the summer at M4, since the wind-mixed layer can be less than 11 m deep for at least short periods of time. This is discussed in more detail in the section entitled *Observations from M2 and M4: Temperature*. The placement of instruments was designed to observe the evolution of the wind-mixed layer, which is typically 20–25 m deep. There are fewer instruments in the lower part of the water column,

since tidal currents result in a well-mixed bottom layer.

Instruments sampled nominally at 10-min to hourly intervals, but over the years M2 has been the site of several process studies in which the sampling was as rapid as every 2 min. Many of the data presented in this manuscript have been low-pass filtered with a 35-h, cosine-squared, tapered Lanczos filter to remove tidal and higher frequencies, and then resampled at 6-h intervals.

Conductivity–temperature–depth (CTD) data were obtained on virtually all recoveries and deployments and used for quality control of the data collected by instruments on the moorings. CTD measurements usually were taken with a Seabird SBE9plus system with dual temperature and salinity sensors. Data were recorded during the downcast, with a descent rate of 15 m min^{-1} to a depth of 35 m, and at 30 m min^{-1} below that. In addition, nutrient and zooplankton data were collected on each cruise in the vicinity of the moorings; these data are not presented in this manuscript.

Weekly data on ice extent and concentration were obtained from the National Ice Center (NIC). The NIC has published a CD of ice extent and concentration from 1972 to 1994. The CD specified ice concentration and extent in 0.25° latitude \times 0.25°

Table 1
The depth of instruments on M2 which collected data is indicated

Date	Temperature	Salinity	Fluor.	CM	ADCP (KHz)
3/14/95–4/30/95	1,10,15,20,26,32,38,44,50,56	10,44	11,44	20,56	150
5/7/95–9/3/95	1,9,15,20,26,32,38,44,50,56	9,26,44,71	10,26,44	20,56	150
2/15/96–4/23/96	7*,11,17,20,25,29,32,35,38,43,49,64	7,11,17,25,43,64	11,25,43	13	600
4/23/96–9/19/96	1,6,12,15,20,24,27,31,34,39,44,50,56,62	1,6,12,15,24,44,62	12		600
9/19/96–2/19/97	10,14,15,20,25,30,35,40,45,55,65	10,55	10	14	150
2/21/97–4/20/97	7*,11,14,17,20,25,29,32,35,38,43,49,54,64	11,17,25,43,64	11,25,43	14	
4/22/97–9/20/97	1,6,11,15,20,24,27,31,34,39,44,50,62	1,6,11,15,24,44,62	11,25,44	8	
9/21/97–2/24/98	10,14,15,20,30,35,40,55,65	10,55	11	14	
2/24/98–4/16/98	7*,11,15,17,20,25,29,32,35,38,43,49,54,64	7,11,17,25,43,64	11,25,43	15	500
4/16/98–6/18/98	1,12,13,15,20,24,27,31,34,39,44,50,56	1,12,13,15,24,44	12,24,44	8	600
7-13-98–10-2-98	1,11,12,15,20,24,27,31,34,39,44,50,56,62	1,11,12,15,24,44, 62	12,24,44	8	600
10/2/98–4/24/99	7*,10,15,20,25,30,35,40,45,55,65,69	10,55	10		500
4/24/99–9/21/99	1,6,7,12,15,20,24,27,31,34,39,50,56,62	1,6,12,15,24,62	12,24	8	
9/21/99–4/25/00	7*,20,25,30,40,55,65,69	55			150
4/24/00–9/20/00	1,6,8,12,15,20,24,27,31,34,39,44,50,56, 62	1,6,12,15,24,44,62	12,24,44	8	600
9/20/00–2/6/01	10,14,15,20,25,28,30,35,38,40,45,55,65, 69	10,55	10		300
2/6/01–5/16/01	13,14,17,20,25,29,32,38,43,49,54,64	13,17,25,43,64	13,25,43	14	600
5/16/01–10/10/01	1,6,8,12,16,24,27,28,39,44,50,56,62	1,6,24,44,62	12	8	600
10/10/01–5/6/02	6,10,11,16,21,24,26,31,36,41,51,61,65	6,51	6	10	300
5/7/02–10/9/02	1,6,8,12,16,18,20,23,25,27,28,31,32,34,39,44,50,56,62	1,6,12,24,44,62	12,24	8	600
10/9/02–3/4/03	11,15,21,26,29,31,36,41,46,51,56,66	11,31	11	15	300
3/4/03–5/14/03	11,15,19,23,27,31,35,40,45,50,55,67	11,31	11,31	15	300
5/14/03–9/28/03	1,6,8,12,16,18,20,24,25,27,28,31,32,34,39,44,50,56,62	1,6,12,24,44,62	12,24	8	600
9/27/03–4/26/04	11,15,19,23,27,31,35,40,45,50,55,67	11,31	11	15	300
4/26/04–9/27/04	1,6,8,12,15,18,21,24,28,32,34,39,44,50, 56,62	1,6,12,24,44,62	12,24	8	300
9/27/04–4/21/05	11,12,15,19,23,27,31,35,40,45,50,55,67	11,31		15	300
4/23/05–9/23/05	1,6,8,12,15,18,21,24,28,32,34,39,44,50, 56,62	1,6,12,24,44,62	12,24	8	300

Instruments that failed completely are not listed. When ship-time was available in February or March, we deployed a single mooring at M2 to measure temperature and salinity near the surface; those series are indicated by an *. The mooring deployed on September 1999, was caught by a fishing net and dragged ~10 km. It was not recovered until almost a year later, without the top instruments. Fluor. refers to fluorometer and CM refers to current meter (RCM-7 or RCM-9). M4 has fewer instruments on it, although its configuration is similar to the winter configuration for M2.

longitude bins. After a break of several years, the NIC began to place ice concentration information in GIS format on their website (<http://www.natice.noaa.gov/pub/Archive/arctic/> and <http://www.natice.noaa.gov/products/archi/index.htm>), and we have now obtained data from 1995 to 2005 from that site and converted it to 0.25° bins. The NIC uses satellite data from Radarsat, DMSP, and Envisat as well as aerial reconnaissance, local information, climatology, and meteorological information, and models to produce their estimates of ice extent and concentration.

Analysis of air–sea interactions over the Bering Sea shelf is based on the synthetic data from the NCEP/NCAR reanalysis (Kalnay et al., 1996). We follow the procedure used in Bond and Adams (2002) to specify particular elements of the atmospheric forcing of the Bering Sea shelf on a daily basis for selected periods. The winds from the

reanalysis are quite reliable in this region (Ladd and Bond, 2002). We also consider air–sea heat fluxes, and while they are expected to be less accurate than the reanalysis of winds, the signals in the Bering Sea are large enough to be meaningful.

3. Results and discussion

3.1. Variability in sea-ice extent, concentration and persistence

Sea ice is a crucial aspect of the physical environment of the Bering Sea. Most of the sea ice forms in polynyas in the northern Bering Sea. Beginning roughly in November, episodic outbreaks of Arctic winds cool the water column, form ice, and advect the ice southward. The leading edge of the ice melts as it is advected over warmer water, rapidly cooling the water column. Maximum ice

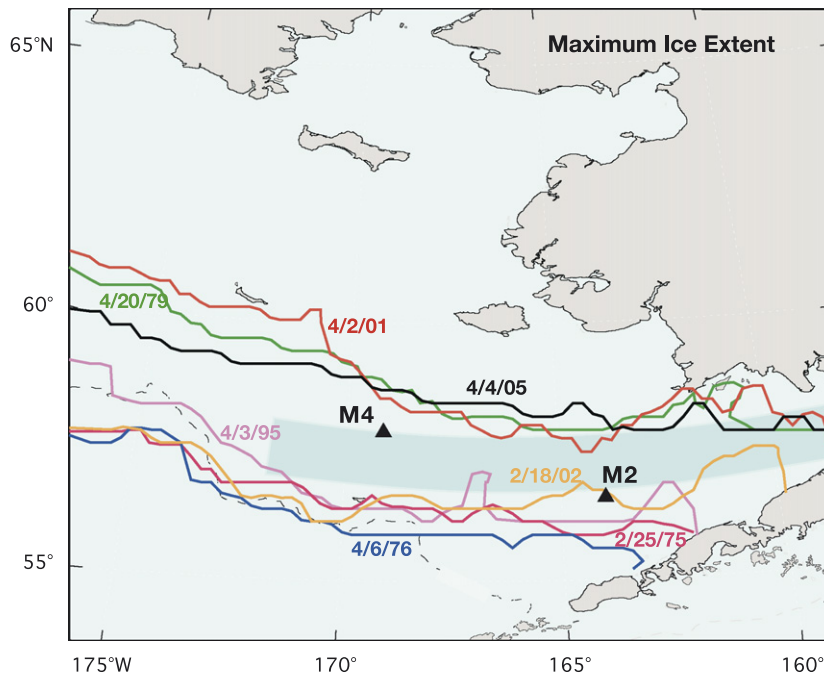


Fig. 2. Maximum ice extent (>5% concentration) during selected years as discussed in the paper. The locations of M2 and M4 are indicated as triangles. The shaded area is the box where ice concentrations shown in Fig. 3 were calculated.

extent has occurred as early as January and as late as May (Fig. 2). Although at maximum extent, sea ice typically covers much of the eastern Bering Sea shelf, there is significant variability in its extent, concentration and duration. Shown in Fig. 2 are the maximum ice extents for 3 years with minimal ice cover (1979, 2001, and 2005) and for 4 years with more extensive ice cover (1975, 1976, 1995, and 2002). As can be seen, maximum ice extent can vary by ~300 km (e.g., 1976 versus 2001).

There are numerous ways of showing the variability in ice extent, each of which reveals different aspects of the spatial and temporal patterns that characterize ice coverage. First, we focus on the average concentration of ice in a 1°-latitude “box” from 57°N to 58°N, and 171°W to the Alaskan coast (shaded area in Fig. 2). M2 is just south of the 57–58°N band and M4 is at its northern edge. The concentration in this band is an index of amount of sea ice present over the southeastern shelf. It is evident that during the pre-1977 “cold regime” (Stabeno et al., 2001), ice was extensive, covering more than 80% of the index area at maximum extent (Fig. 3). This 5-year period in the early 1970s was anomalously cold, with more extensive ice than in the 1950s and 1960s, although data records from this earlier period are limited. In

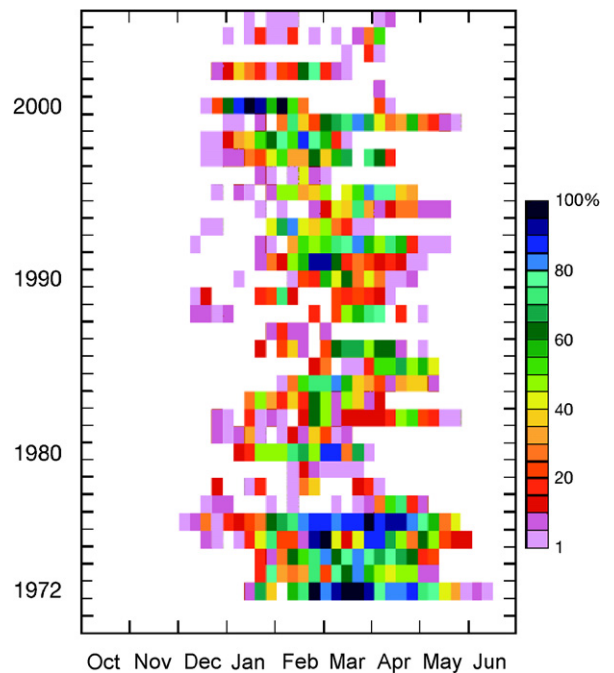


Fig. 3. Percent ice cover from 57°N to 58°N (the shaded area in Fig. 2). Each square represents 1 week.

addition, ice in the early 1970s persisted for months over the southeastern Bering Sea shelf. For instance, in the early 1970s ice was present in concentrations

above 70% for 4–5 months. During the last three decades, there has been a marked decrease in ice extent, duration and concentration over the south-eastern Bering Sea, with 2001 often characterized as having the smallest ice extent ever recorded over the shelf. The 5 years (2001–2005) since 2000 also have been characterized by low concentrations of ice. Specifically, there has been no period where ice concentration in the index box exceeded 70%, and the duration of significant amounts of ice (concentrations >25%) in the box has been at most a couple of weeks.

Not only has the ice concentration changed, but the character of the ice advance has also changed

during the last 6 years compared with the period 1989–1999 (referred to as the “cool period” in Stabeno and Hunt, 2002). In the “cool period”, ice advanced steadily with little variability from year to year (Fig. 4A). During the last 6 years, the year-to-year variability in ice advance has been marked (Fig. 4B), and in 4 (2001, 2003, 2004, and 2005) out of 6 of the years, ice arrived much later than in the cool period of the 1990s. The ice retreat in the southern part of the shelf (south of 59°N) mostly occurred earlier than during 1989–1999. However, the retreat of ice over the northern shelf has been highly variable, with ice persisting longer in 2001 than was common in 1989–1999.

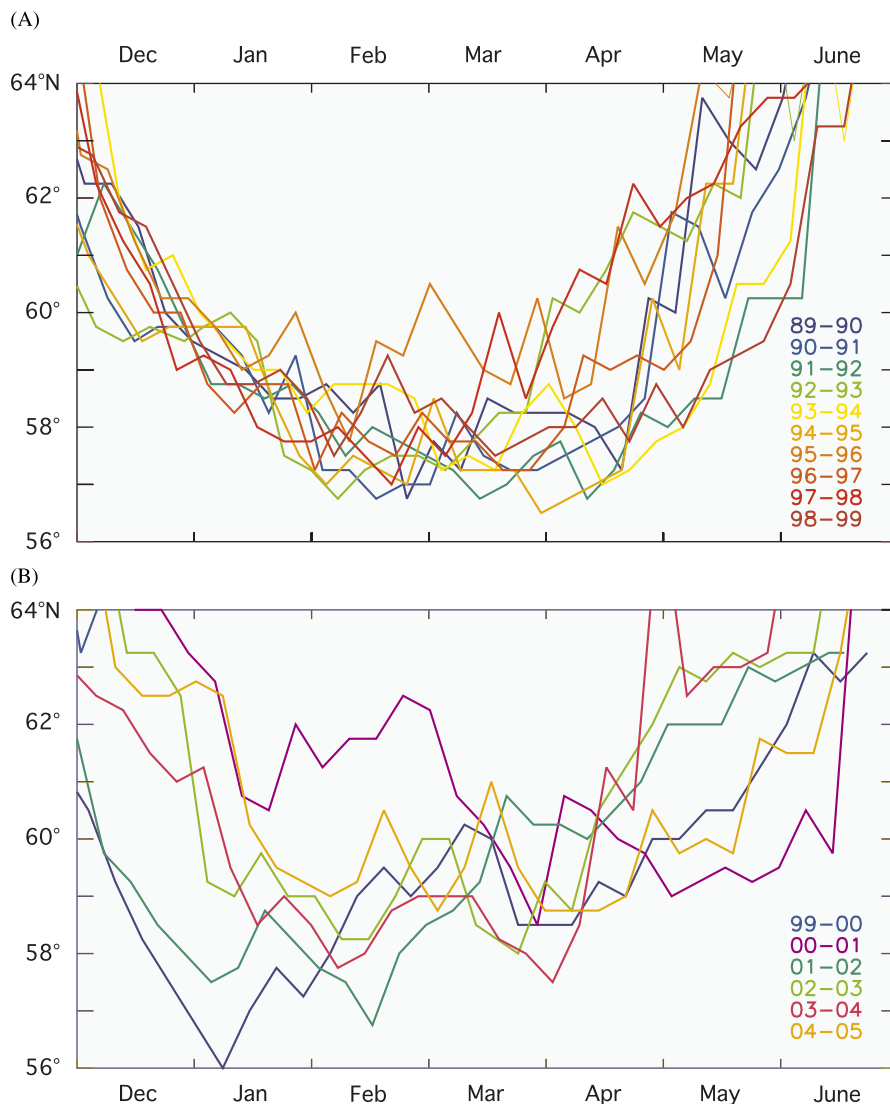


Fig. 4. The southernmost latitude of sea ice along 169°W during each week from December to June. The upper panel represents the “cool period” years from 1989 to 1999 and the bottom panel the warmer period that has dominated the system during the last 5–6 years.

The decadal shifts in sea-ice concentration coincide with changes in large-scale decadal patterns such as the PDO and AO. The PDO is the first mode of decadal variability in the North Pacific sea-surface temperature (SST). Phase shifts, often called regime shifts, occurred in 1947 and 1976 with a shift of the PDO time series from positive to negative, and negative to positive, respectively (see Fig. 5 in Bond et al., 2003). In 1989, the decadal variability of the North Pacific appeared to undergo a mode shift, with the second mode of SST variability (the Victoria Pattern) becoming more prominent and the first mode (the PDO) becoming less so. This resulted in the Victoria Pattern accounting for more variance than the PDO during the last decade and a half (McKinnell, 2004). In conjunction with shifts in the PDO in 1947 and 1976 and the strengthening of the polar gyre (AO) in 1976, there was a marked shift in the magnitude of some fish populations (Hare and Mantua, 2000). It is important to note that the PDO is an indicator of variability of the North Pacific and not the forcing mechanism of regime shifts. It is largely changes in the atmosphere that force changes in the SST. The mechanisms that cause these shifts in the atmosphere are not completely understood, nor is the role that the ocean plays in these atmospheric shifts.

In addition to decadal variability, sea-ice concentration and extent also vary on year-to-year time scales. For instance, changes in ENSO are weakly correlated with ice extent (Niebauer, 1988), with a tendency for an El Niño to be accompanied by less extensive ice in the Bering Sea (Stabeno et al., 1998). As shown by Rodionov et al. (2007), these correlations are weak because interannual variations in the wintertime conditions on the Bering Sea shelf are most closely related to regional anomalies in the atmospheric circulation.

A decrease in sea ice directly impacts water-column temperature and salinity. As the leading edge melts, it quickly cools the water column to the freezing point (approximately -1.7°C) and freshens it. Depending upon when and how the ice retreats, it leaves behind different water-column signatures. If the ice melts or is advected away slowly, and there are no strong storms after its retreat, the surface layer will be fresher than the near-bottom water. As the water warms during the spring, the salinity gradient contributes to the strength of the density difference between the top and bottom layers, thus damping mixing over the middle shelf during summer. What usually occurs over the southeastern

shelf, however, is that winds transport the ice northward off the southern shelf, and the combination of winds and surface heat fluxes is sufficient to maintain a quasi-isothermal water column prior to seasonal warming. With or without stratification due to salinity, spring and summer atmospheric heating results in a warm, surface-mixed layer. The strong density gradient then insulates the cold bottom layer from heating throughout the summer. This bottom layer is referred to as the cold pool (if temperatures are less than 2°C) or the cool pool (if bottom temperatures are greater than 2°C).

Ocean temperatures have profound influences on the distribution of many species of fish. For instance, walleye pollock (*Theragra chalcogramma*) tend to avoid water below 2°C (e.g., Wyllie-Echeverria, 1995; Overland and Stabeno, 2004). Species such as Arctic cod (*Boreogadus saida*) that prefer cold temperatures have retreated to the northern portion of the Bering Sea.

The sea ice over the shelf also determines the timing and nature of the spring phytoplankton bloom (Stabeno et al., 1998, 2001; Hunt et al., 2002). When ice is present after mid-March there tends to be a spring phytoplankton bloom in the marginal ice zone. In contrast, when sea ice is absent or retreats before mid-March, the spring phytoplankton bloom does not occur until after set-up of thermal stratification (Stabeno and Hunt, 2002).

3.2. Observations from M2 and M4

3.2.1. Temperature

A decade of observations at M2 have expanded our understanding of the Bering Sea ecosystem, in particular the physical and chemical (bottom-up) mechanisms that control primary production. In Fig. 5A and B, temperatures were extrapolated from the upper thermistor to the surface if that thermistor was at or above 11 m. At M2 during the spring/summer months (April–September), temperature was measured at ~ 1 m. During most years, the surface mooring, with a thermistor at 1 m, was deployed in April and recovered in September or early October. The average difference between temperatures measured at 1 m (T_1) and those measured at 11 m (T_{11}) was less than 0.03°C in April, September and October. During November through March, the wind mixed layer is greater than 10 m, so the thermistor at 11 m is a good estimate of surface temperature. Noting this, a similar conclusion can be made for M4: from September through

April, temperature measured at 11 m is a good estimate of surface temperature. For M4 during summer, the best estimate of how surface temperatures compare to those at 11 m comes from an examination of temperature differences at M2. At M2, the average temperature difference ($T_1 - T_{11}$) during August (1995–2005) was 0.13°C and during May was 0.27°C . The differences in June and July were larger, 0.69 and 0.44°C , respectively. These larger differences are largely caused by particularly weak winds during specific years. For instance, June 1997 was particularly calm, and 20 of 40 days where $T_1 - T_{11}$ exceeded 2°C were in that month. Similarly, 9 of the 40 days where $T_1 - T_{11}$ exceeded 2°C were in July 2004. Most of the other times when $T_1 - T_{11} > 2^\circ\text{C}$ were single calm days. So for June and July, using temperatures at 11 m as an indication of surface temperatures at M4 can be an underestimation.

The temperature records (Fig. 5) from the moorings at M2 and M4 reveal a well-defined seasonal cycle that is typical for the southeastern middle shelf. In January, the water column is well mixed. This condition persists until buoyancy is introduced to the water column either through ice melt or springtime (predominantly solar) heating. The very cold temperatures ($< -1^\circ\text{C}$; indicated by black in Fig. 5) that occurred in 1995, 1997, and 1998 at M2, and in 1997 and 2002 (to a lesser extent in 2003 and 2004) at M4, resulted from the local melting of ice. Generally, once stratification develops during April, the water column exhibits a well-defined two-layer structure that is characteristic of the middle shelf (water depths 50–100 m) throughout the summer, typically consisting of a 15–35 m wind-mixed layer and a 35–45 m tidally-mixed bottom layer. This bottom layer is the cold or cool pool. In earlier years (1995, 1996, 1997, and 1999) the bottom temperatures were below 2°C , but in more recent years bottom temperatures have been much warmer, indicating no formation of the southern cold pool. Deepening of the mixed layer by strong winds begins as early as mid-August, and by early November the water column is again well mixed.

At M2, the coldest summer SSTs occurred in 1999 (Fig. 5), which had a late ice retreat (Fig. 3). The warmest summer SST occurred in 2004, when temperature in the wind-mixed layer exceeded 12°C for over 2 months. Bottom temperatures were coldest in years when ice was present during the spring. Typically, the temperature of the wind-

mixed layer increased by $\sim 10^\circ\text{C}$ during the late spring and summer, while bottom temperatures, insulated by the sharp density gradient, warmed by only a few degrees during the same period.

The depth-averaged temperature was calculated using temperature time series measured at M2 and M4 (Fig. 6). The errors in these estimates at M2 are small, but during the summer at M4 the underestimation of average temperature is larger. For instance in June when the monthly average $T_1 - T_{11}$ is 0.69°C , the depth-averaged temperature at M4 would be underestimated by $\sim 0.1^\circ\text{C}$ and in particular months it could even be larger. For instance, in July 2004 the monthly average temperature was underestimated by $\sim 0.3^\circ\text{C}$.

As expected, a strong annual signal is clearly evident in the time series, as is the marked warming at M2 that occurred in 2000. Recall that the location of M2 was chosen because historically ice occurred over this site for a few weeks virtually every winter. This pattern of ice being advected over the M2 site and cooling the water column continued from 1995 to 2000, but from 2001 to 2005 no ice (that is, ice areal concentration was less than 10%) covered the M2 site, although in 2002 the edge of the ice was very close to the mooring. This lack of sea ice has contributed to the sharp warming of $\sim 3^\circ\text{C}$ in the winter and $\sim 2^\circ\text{C}$ in the summer at M2.

Unfortunately, the record at M4 is too short to identify clearly a shift in temperature, although the limited data collected there in 1997 (Fig. 5B) show much colder winter conditions than observed after 2000. The ice extent in 1997 was fairly typical of the 1980s and 1990s (Fig. 3), which suggests that temperatures at M4 also would have undergone a warming in 2000 with the reduction in ice extent. M4 is farther north than M2, and therefore is exposed to more extensive ice cover and colder ocean temperatures, at least during the winter, than occurs at M2. Colder temperatures were clearly evident in 2002, when ice covered M4 sporadically for 2–3 months, but did not reach M2. Interestingly, during the spring and summer, ocean temperatures are not always warmer at M2 than M4 (e.g., late spring and early summer 1999 and 2000 in Fig. 6).

It has been observed previously that during years of extensive ice cover, the southern cold pool (centered on M2) can be separate from the northern cold pool (north of 59°) (Schumacher and Stabeno, 1998). The water column near M4, which lies in the broad boundary between the southern and northern cold pools, appears to be modified by a weak, local

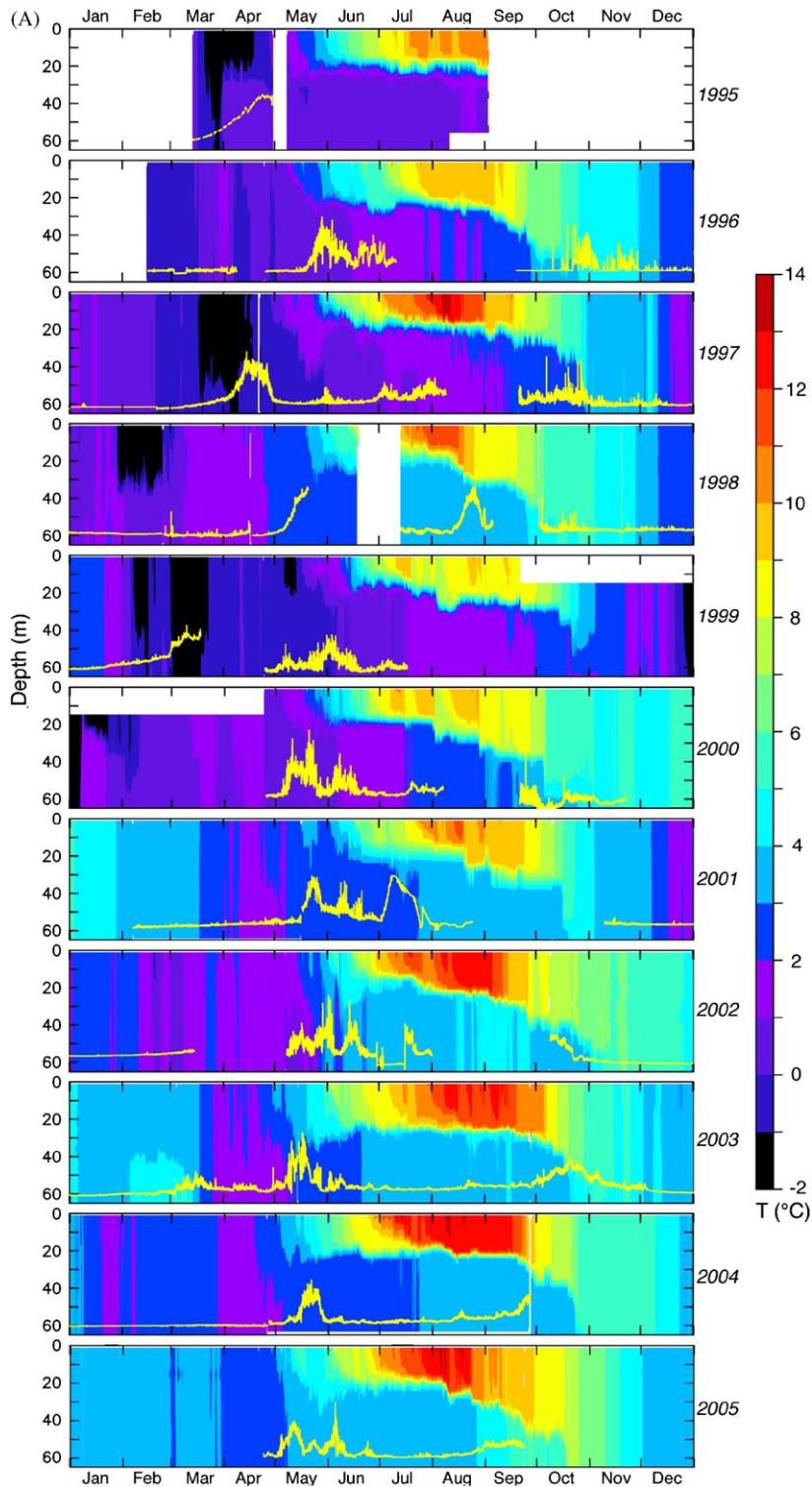


Fig. 5. (A) Contours of temperature measured at M2. The coldest temperatures (black) occurred when ice was over the mooring. The temperature contours have been extended to the surface from 10 m during winter (October–March) period as discussed in the text. The yellow line is fluorescence measured at ~11 m. Note that early blooms are associated with the presence of ice. (B) Contours of temperature measured at M4. The coldest temperatures (black) occurred when ice was over the mooring. The temperature contours have been extended to the surface from ~10 m as discussed in the text. The yellow line is fluorescence measured at ~11 m. Note that early blooms are associated with the presence of ice.

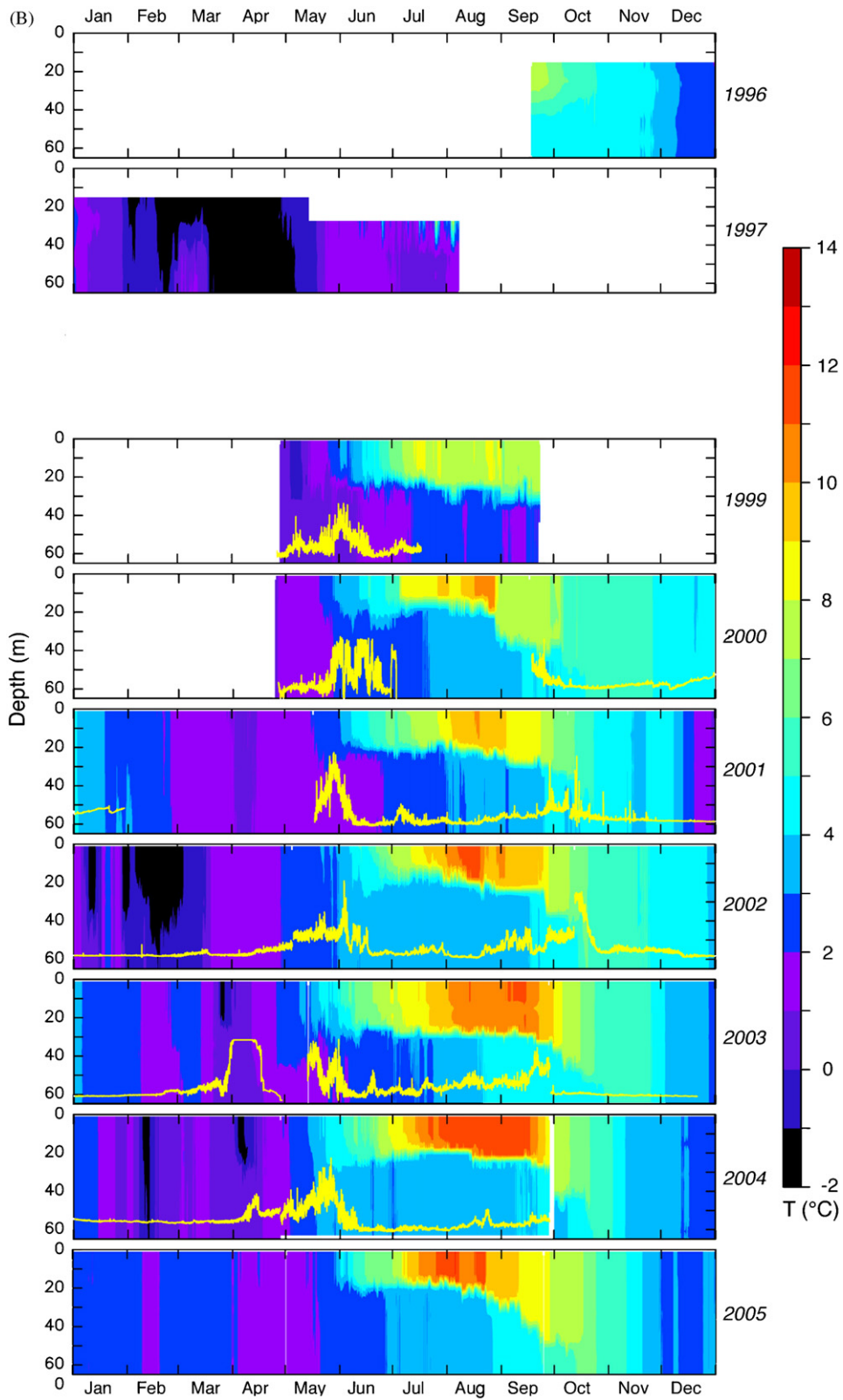


Fig. 5. (Continued)

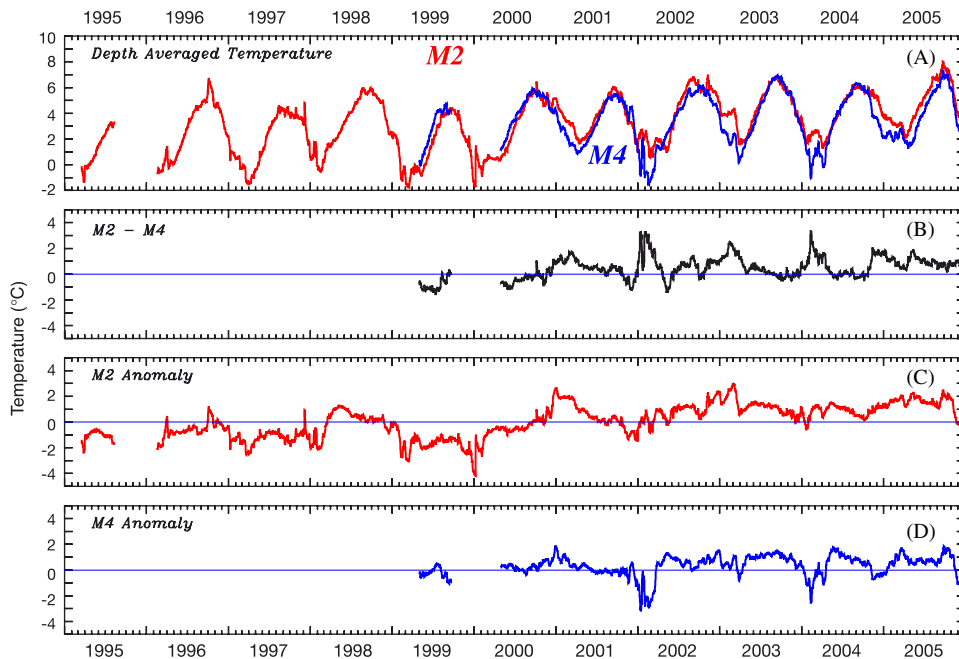


Fig. 6. (A) Depth-averaged temperature at M2 and M4. (B) The difference between depth-averaged temperatures at M2 and M4. The depth-averaged temperature anomaly (the seasonal signal has been removed) at (C) M2 and (D) M4. All time series have been low-pass filtered.

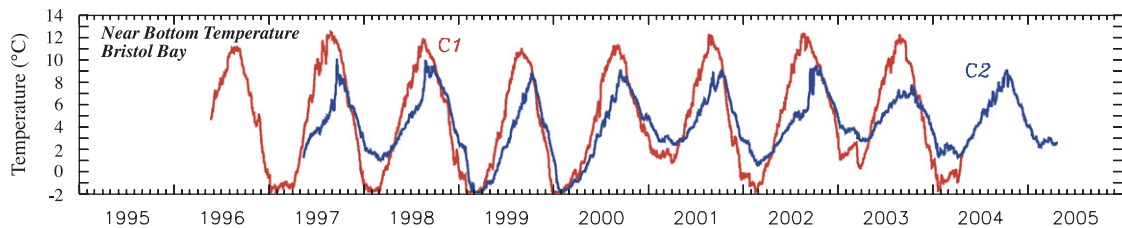


Fig. 7. Near bottom temperatures at the two moorings in Bristol Bay. C1 is in 20 m of water and C2 in 60 m. The time series have been low-pass filtered.

cross-shelf flow. This flow is likely an extension of the flow around the Pribilof Islands. Significant anti-cyclonic flow occurs around the Pribilof Island (Stabeno et al., 2002a; Kowalik and Stabeno, 1999), and some of this flow continues eastward across the shelf at $\sim 57.5^\circ\text{N}$ (Schumacher and Stabeno, 1998; Stabeno et al., 2001). Thus M4 may be warmed by weak flow that originates along the slope of the Bering Sea. However, from an examination of the currents in Section 3.2.2 below, this is not clear.

The trend of warming over the shelf is clearly evident when the annual cycle has been removed (Fig. 6C and D). At M2, from 1995 to 1997, depth-averaged temperatures were 1–2 °C cooler than the mean, except for a month-long warming that occurred in September 1996 as a result of advection. Depth-averaged temperature was above average in

1998, and then cooled again in 1999 and 2000. Since then conditions have largely been warmer than the 10-year seasonal cycle. The warm anomalies have been slightly greater in winter ($\sim 3^\circ\text{C}$) than in summer ($\sim 2^\circ\text{C}$). Using an annual signal from just 1999 to 2005 at M4, the temperature anomalies there also show some indication of warming during the summers, although winter conditions are highly variable and clearly dependent upon the presence (or absence) of sea ice.

Farther to the southeast near the Alaska Peninsula, the near-bottom temperatures at C1 and C2 also show a strong seasonal signal (Fig. 7). The water column at C1 (water depth $\sim 20\text{ m}$) is well mixed because of strong tidal currents. C2 (water depth $\sim 60\text{ m}$) is well mixed during the winter, but has a two-layered structure during the summer. The water column at

C1 responds quickly to atmospheric forcing, resulting in warmer temperatures during the summer and cooler temperatures during the winter than at C2. These moorings were first deployed just 1 year later than the first deployment at M2. Temperatures at C1 and C2 show a pattern similar to that at M2 with warmer winter conditions dominating since 2000. Thus, it is likely that the conditions observed at M2 and M4 are representative of much of the middle shelf south of St. Matthew Island.

The moorings in Pavlof Bay (P1; Fig. 1) in the Gulf of Alaska show a very similar pattern to that observed in the southeastern Bering Sea (Fig. 8). As in the Bering Sea, the winter temperatures of 1999 and 2000 were colder than temperatures from 2001 to 2005, with the summer of 2004 particularly warm.

This site is interesting, even though it is not in the Bering Sea, in that the temperature was modified by large scale climate patterns that affected both the Bering Sea and the Gulf of Alaska, and perhaps by local atmospheric forcing. The water at Pavlof Bay and along the south coast of the Alaska Peninsula eventually passes through Unimak Pass and into the Bering Sea (Stabeno et al., 2002b).

3.2.2. Mean currents and winds

The measurements at M2 and M4 also include currents. The low-pass filtered currents from 2001 to 2002 are characteristic of the variability in currents at M2. While currents are weak in summer (Stabeno et al., 2002a), during fall they become more energetic (Fig. 9) not only at the surface, but also

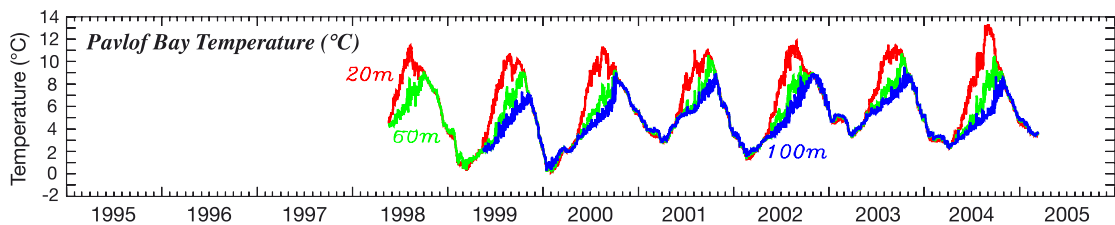


Fig. 8. Temperature at three depths (20, 60, and 100 m) at the entrance to Pavlof Bay in the Gulf of Alaska (P1 in Fig. 1). The time series have been low-pass filtered.

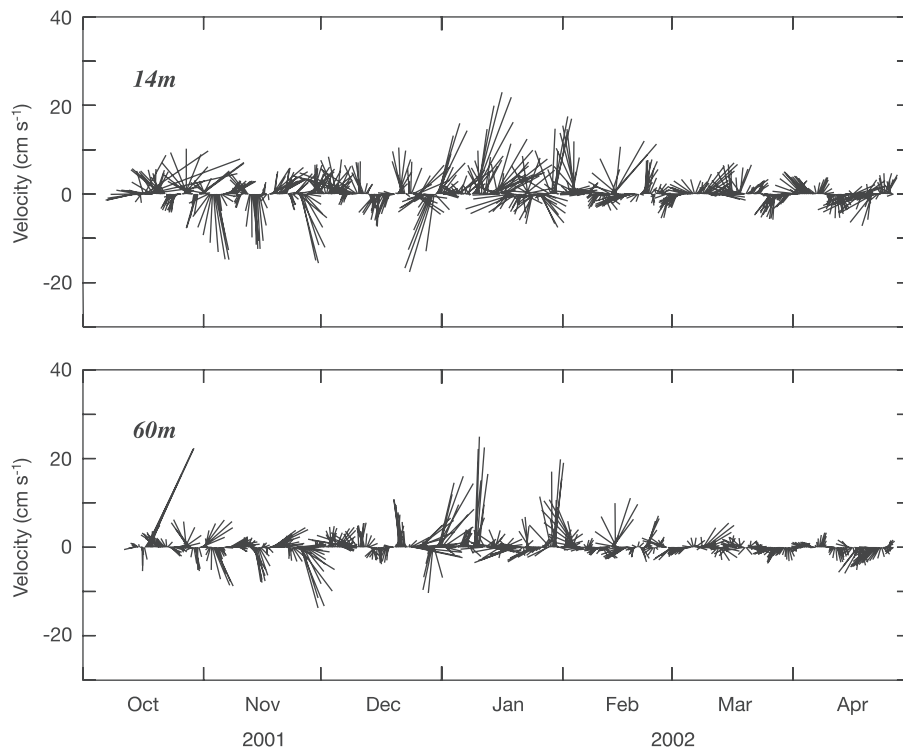


Fig. 9. Low-pass filtered current velocity measured at 14 and 60 m depth at M2. Up is northward flow.

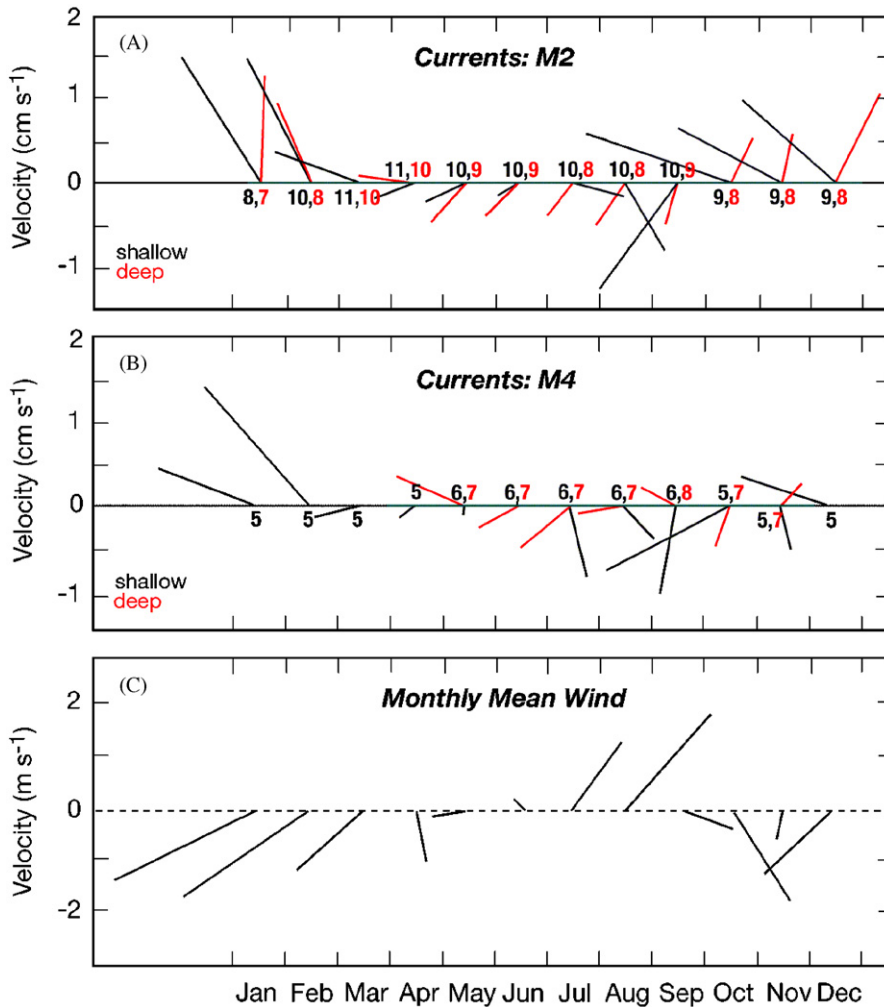


Fig. 10. The mean monthly current velocity (A) at M2 and (B) at M4. The shallow currents were measured at depths of 8–12 m and the deep currents were measured at 55–65 m. The numbers along the axis indicate the number of years that there were data during that month. (C) The NCEP reanalysis wind velocity has been interpolated to the position of M2. Up is northward flow.

near the bottom of the water column. These stronger currents persist into the winter. Although the low-pass filtered currents can be fairly energetic, exceeding 10 cm s^{-1} for several days, the monthly mean flow tends to be sluggish (Fig. 10A).

The length of the record at M2 is now sufficient to resolve the mean seasonal cycle in currents at that site. From October to March, monthly mean currents in the upper water column are $> 1.5 \text{ cm s}^{-1}$ (except in March), and have a northward component (Fig. 10A). The flow near the bottom is weaker, but also has a northward component during the winter. During the remaining 6 months, the monthly mean flow is weaker with a southward component. The time series at M4 is shorter

than that at M2, but they show a similar pattern (Fig. 10B). The strongest flows are in January and February, with a northward component during November through February. During the remainder of the year the flow has a weak southward component. It is interesting that there is no evidence of eastward flow in the monthly means at M4, as was observed in satellite-tracked drifter trajectories (by Reed and Stabeno, 1996). They hypothesized that such a flow could explain the warming that occurs at M4.

The mean monthly winds (from NCEP/NCAR Reanalysis) also feature a well-defined annual cycle: southwestward winds ($\sim 2 \text{ m s}^{-1}$) from December to March weaken during spring and shift to

northeastward in July and August (Fig. 10C). During months with stronger mean winds (January–March, August, November, and December), the currents in the upper water column are 80–120° to the right of the wind. While the near-surface currents at M2 may be influenced by Ekman dynamics at times, it is clear that other dynamics play a critical role in forcing the currents over the shelf. They are likely forced by more regional effects, presumably in combination with local baroclinicity.

3.2.3. Fluorescence

The timing of spring primary production on the southern Bering Sea shelf is determined by a combination of the date of ice retreat, solar heating and wind mixing. If the ice retreat is late, i.e. after mid-March as occurred in 1995 and 1997, an early phytoplankton bloom occurs under the ice in cold water (Fig. 5). With an early ice retreat as occurred (1996 and 2000) or during winters that are ice-free (2001–2005), the bloom occurs later, in May or even June, when surface heating due to insolation provides the necessary ocean stratification.

Time series from M2 and M4 have documented this process. The fluorescence (depth ~11 m), shown in Fig. 5, is an indication of the timing of the phytoplankton blooms (enhanced fluorescence), not an indication of production rates. All the time series have been normalized so that the maximum peaks are of similar magnitude. At M2, the ice-associated bloom consumes all the nutrients in the upper water column (Stabeno et al., 2002a), preventing a later spring bloom, although episodes of higher fluorescence will occur during summer storms (e.g., August 1998) that entrain water from the nutrient-rich bottom layer. The fall is often characterized by an increase in fluorescence that corresponds to the break down of the strong two-layer structure that characterizes the middle shelf during summer.

It has long been hypothesized that an early spring phytoplankton bloom results in a mismatch between peak phytoplankton biomass and zooplankton grazing, and results in higher flux of carbon to the seafloor and a smaller copepod biomass compared to years with early ice retreat (Hunt et al., 2002). It also results in a mismatch between larval pollock and their prey (Napp et al., 2000). While there is evidence to support these hypotheses over the southern shelf (Hunt et al., 2002; Napp et al., 2000), there is less information over the northern shelf (north of St. Matthew Island).

3.3. Possible causes of warming over the southeastern shelf

The warming over the southeastern shelf is closely interwoven with the absence of sea ice, but it is not clear whether it is solely changes in atmospheric patterns that have resulted in a decrease in ice and in warming, or whether the ocean plays a role. We will explore four mechanisms in this section. First, changes in the winter winds directly affect both the temperature of the Bering Sea shelf and the formation and advection of sea ice, but it is not solely *wind direction* that influences ice formation. The origin of the air itself impacts ice formation, since frigid air temperatures are a necessary condition for the creation of sea ice (Stabeno et al., 2001; Bond and Adams, 2002; Rodionov et al., 2007). Second, shortening of the ice “season” through a later fall transition and/or an earlier spring transition can limit the southern extent of the ice. The third mechanism is a feedback effect: the presence of warmer shelf water during summer (due to a lack of ice the previous winter) results in warmer fall temperatures, which would delay the advection of ice by increased melting of the leading edge. Finally, changes in the flow through Unimak Pass during winter can contribute to increased wintertime ocean temperatures over the southeastern shelf, which also could delay the advection of ice.

These mechanisms interact in complex ways and are not independent of each other. Quantitative evaluation of these interactions is best accomplished using numerical ocean models. For the present study, however, we use a combination of discussion of earlier studies, simple models and a comparison between 2 years, 1975 and 2002, to help illustrate the effects of the mechanisms introduced above. The years 1975 and 2002 were chosen to assist in this exploration because they had similar winter weather conditions overall, but decidedly different ice extents and ocean temperatures the previous fall.

3.3.1. Comparison of 1975–2002

To prepare for the discussion in the following four sections, we begin by showing the mean atmospheric circulation for the two winters. The 700 hPa geopotential height anomaly maps for December–March of the winters of 1975 and 2002 (Fig. 11) both include lower than normal heights over the northern Bering Sea and higher than normal heights over the central North Pacific south

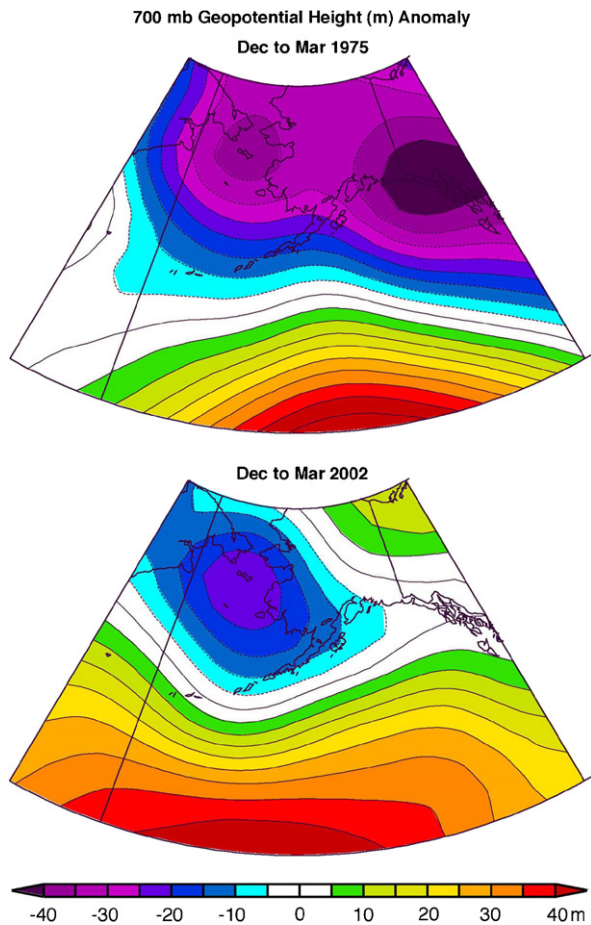


Fig. 11. Mean 700 hPa geopotential height anomaly (m) for (top panel) December 1974–March 1975 and (bottom panel) for December 2001–March 2002. Anomalies are relative to a baseline period of 1968–1996.

of the Aleutians, implying in each case relatively strong eastward flow aloft. This anomalous westerly flow off the eastern tip of Siberia brought about lower tropospheric air temperature anomalies of approximately -3°C in 1975 and approximately -1°C in 2002 in an east–west band across the Bering Sea (not shown). While the overall weather pattern was similar for the two winters, it is instructive to examine two aspects of the air–sea interaction in greater detail. Daily time series of the net surface heat fluxes in the southern Bering Sea for 1975 and 2002 (Fig. 12A and B) show the character of the sub-seasonal fluctuations in the surface heat exchange. Through February, both years had substantial loss of heat from the ocean to the atmosphere. In 1975, however, there was one additional outbreak of cold arctic air in March.

In both years, the maximum ice extent over the western portion of the shelf was similar, covering most of the slope and outer shelf. Over the eastern portion of the shelf, however, the ice cover was more extensive in 1975 than in 2002 (Fig. 2). Maximum ice extent occurred in February in both years (Figs. 2 and 3). Although the negative heat fluxes through February were larger in 2002, the maximum ice extent was greater in 1975. In addition, the cooling event in mid-March resulted in persistence of ice over the shelf in the 1975 compared with 2002 (Fig. 3).

3.3.2. Changes in wind direction and air mass (Mechanism 1)

There is a direct link between strong, arctic winds which blow southward and the formation of sea ice. These frigid winds are critical not only in the formation and advection of ice, but also in cooling of the water column before the arrival of ice. The atmospheric circulation patterns that result in extensive ice are complex (e.g., Rodionov et al., 2007), but some general statements can be made. Patterns that pump warm, maritime air northward into the Bering Sea and then southward over the eastern shelf do not produce extensive ice, while patterns in which cold, arctic air blows southward typically result in extensive ice formation (Stabeno et al., 2001; Bond and Adams, 2002). We discuss both the winter and spring atmospheric patterns here, as have been discussed in several recent publications.

The atmospheric circulation during the winters since 2000 has favored relatively low sea-level pressure (SLP) over the Bering Sea (Overland and Wang, 2005b). While the meridional component of the winds has been fairly typical in this period, there has been reduced cooling of the ocean by the atmosphere. The lower SLP over the Bering Sea signifies a greater proportion than usual of the warm and moist air masses of maritime origin that accompany cyclonic disturbances, and a reduced frequency of cold and dry air masses of continental or arctic origin that accompany high-pressure anticyclones (e.g., Stabeno et al., 2001; Bond and Adams, 2002).

Such a change in air temperature not only directly impacts the formation of sea ice, but it also influences the cooling of the water column. As can be seen in Fig. 5, the winter ocean temperatures at M2 from 2000 to 2005 have been several degrees warmer than ocean temperatures from 1996 to 2000.

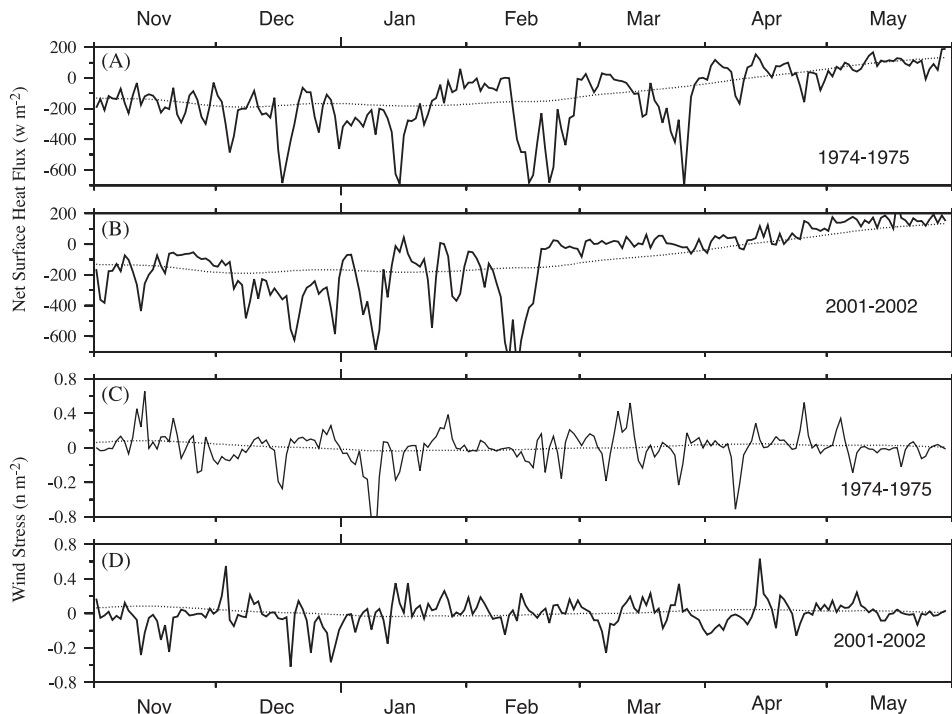


Fig. 12. Daily values of the net surface heat flux (W m^{-2}) at (A) Site 2 (57°N , 164°W) and (B) at Unimak Pass (54°N , 165°W). Panels (C) and (D) show the along-peninsula wind stress (N m^{-2}) for the same locations for 1 November 1974–31 May 1975. Negative is toward the west-southwest. The dotted lines represent climatological means.

This has been true in December and January, even before ice arrived at the mooring. The lack of cold winds out of the north during late fall and early winter contributed to these warmer ocean temperatures. It is not clear, however, whether the water column has been warmer because of warmer fall winds, or because of the higher heat content in the water column from the previous summer.

A somewhat different mechanism has been operating recently during the spring. As shown by Overland and Wang (2005b), the atmospheric circulation in spring since 2000 has repeatedly featured low pressure over Siberia and high pressure over Alaska. The consequence of this has been northward wind anomalies over the Bering Sea and hence both relatively warm air and anomalous northward transport of sea ice. The impact of these anomalously northward winds has contributed to the early disappearance of ice over the southern shelf (Fig. 3) compared with the 1990s and earlier. The patterns of high and low-pressure anomalies are clearly related to large-scale atmospheric circulation (Overland and Wang, 2005b). As these patterns relax, it is expected that the Bering Sea will become cooler.

3.3.3. Warmer temperatures over the southeastern shelf (Mechanism 2)

There are three primary mechanisms that can cool the water column over the southeastern Bering Sea shelf: direct heat loss to the atmosphere; the horizontal transport of cold water into the region; and the cooling of the water column through ice melt.

We have already discussed the first of these mechanisms: the similar rates of cooling early in the winter season in 2002 and 1975 (Fig. 12A and B). The summer ocean temperature during 2001 was particularly warm (Fig. 5), and this could have contributed to the ice extent in February 2002 being less than that in February 1975. In addition, 1975 had a period of strong cooling after mid-March. These arctic-air outbreaks are particularly effective at producing and advecting ice near the end of winter, when the water column is already near the freezing point.

While the transport of cold water southward could in theory be very effective in cooling the water column, it fails to do so for a couple of reasons. First, there is great variability in the direction and magnitude of currents (Fig. 9). Second, during the

winter, the mean monthly transport at M2 is northward (Fig. 10A), so, on average there is northward flux of heat over the shelf during winter. Episodic advective events, however, do play a role in changing the temperature of the shelf. The sudden warming of the water column by more than 1 °C when ice recedes from the mooring site (e.g., the sudden change from −1.7 °C indicated by black during several years) is evident in Fig. 5A. This is especially clear in January 2000, when the ocean temperature quickly warmed by >2 °C.

The latent heat flux due to the melting of ice is probably one of the most effective ways of cooling the water column. Consider a simple box model with a 70-m-deep water column; melting a 1-m thickness of ice will cool that column by ~1.1 °C. Ice is typically advected at ~2% of the wind speed, so during a day with wind speeds of $V \text{ m s}^{-1}$, ice would be pushed ~2V km (if it did not melt). However, it does melt, and the warmer the water the more rapidly the ice melts. For example, in water 1.1 °C above 0 °C, the 1 m of ice would melt, so that the ice edge would advance only ~V km in a day. If the water column was 2.2 °C above 0 °C the ice edge would advance by 0.67V km in a day. These are just simple estimates to show the impact of warmer water on the ice extent, since ice does not melt instantaneously when advected over warmer water. Warm water can delay the advance of sea ice, but the advance itself is still dependent upon the wind.

3.3.4. Shorter ice season (Mechanism 3)

A delay in the fall atmospheric transition and/or an earlier spring atmospheric transition will result in a shorter ice season. During summer, winds over the southeastern Bering Sea are northward, introducing warmer air masses over the Bering Sea (Fig. 10C). For ice to form, the winds must first shift to southward. In four of the last 5 years, ice has arrived later than it did in the 1990s (Fig. 4), indicative of a later fall atmospheric transition. An earlier spring transition was discussed in Overland and Stabeno (2004). Cold temperatures in spring are more effective in creating the cold pool than are cold conditions in winter, since if ice retreats early strong storms can mix and advect water onto the shelf warming the cold pool (e.g., 1998, Fig. 5A). Using the examples of 1975 and 2002, recent winters have tended to be shorter (rather than milder) than those of the past. The degree to which these regional effects are related to changes in the seasonality of the large-scale atmospheric circulation is unknown.

Certainly, an early transition in 2002 to spring-time conditions contributed to warmer, near-bottom temperatures at M2, when compared with conditions in 1975.

3.3.5. Increases in the transport of heat onto the southeastern shelf (Mechanism 4)

One possible interpretation of the lack of sea ice along the Alaska Peninsula since the mid-1990s is that warmer water is being advected northeastward along the peninsula (see Fig. 2; and Fig. 5 in Stabeno et al., 2002b). The flow through Unimak Pass is an important source of nutrients for the southeast shelf (Stabeno et al., 2002b) and also may represent a significant source of heat. Stabeno et al. (2002b) showed that the transport through Unimak Pass is strongly correlated with the local along-peninsula component of the wind. Southwestward winds confine the Alaska Coastal Current (ACC) along the south side of the Alaskan Peninsula. When so confined, much of the ACC will flow through Unimak Pass, the first (easternmost) broad pass in the Aleutian Arc that the ACC encounters (Nof and Im, 1985). Once through the pass, the flow bifurcates (Fig. 13) with part flowing northwestward along the 100-m isobath and a portion flowing northeastward along the Alaska Peninsula (Stabeno et al., 2002b). Unfortunately, there are limited observations of how strong this eastward flow along the peninsula is during the winter, and even during spring and summer it is only a few centimeters per second.

The time series of the along-peninsula component of the wind stress (Fig. 12C and D) indicate that, due to the winds, northward transports through Unimak Pass were probably larger in the early winter of 2002 than in 1975. Specifically, the mean along-peninsula wind stress was -0.04 N m^{-2} in November–December of 2001 and 0.03 N m^{-2} in November–December of 1974. If we consider just the period when M2 has been occupied (1995–2006), the overall warmth of the shelf in recent years (2001–2005) as compared to the earlier 6 years is consistent with the anomalous westward winds, (due to a stronger than normal Aleutian Low) that have prevailed over the same period.

In addition, ocean temperatures in the Gulf of Alaska near Seward have increased over the last 30 years by ~1 °C (T. Royer, personal comm.). The temperature along the south side of the Alaska Peninsula, as observed at Pavlof Bay mooring (Fig. 8), is warmer since 2001 when compared to

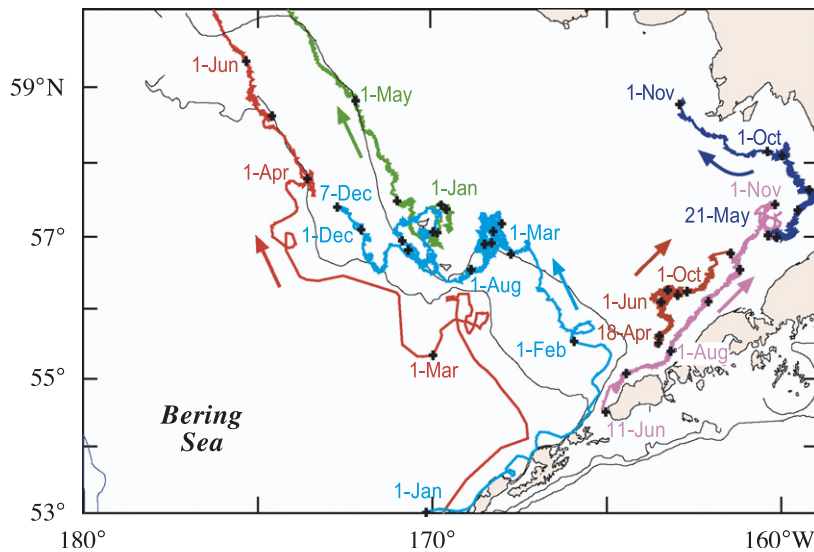


Fig. 13. Satellite-tracked drifter trajectories. The black “+” indicate the position of the drifter at the first of each month. The drifters each had “holey sock” drogues centered at ~40 m depth.

the five previous years. The reason that Pavlof Bay temperatures mimic those at M2 is likely that both are affected by the large-scale atmospheric forcing, plus some “spillover” of the more regional forcing in the Bering Sea. For instance, if sea ice occurs along the north side of the Alaska Peninsula, then winds blowing from the north across the ice would be colder, cooling water along south side of the Alaska Peninsula where the terrain is flat, as it is in the vicinity of Pavlof Bay.

It appears that warmer water is flowing through Unimak Pass, either as a result of general warming of the Gulf of Alaska or local lack of cooling along the south side of the peninsula (e.g., Pavlof Bay). These warmer temperatures together with enhanced northward transport through Unimak Pass could contribute to the observed warming over the southeastern Bering Sea shelf during either the fall or winter. If the eastward flow persists during winter, then it would introduce warmer water along the peninsula, thus limiting the advection of ice over the southeastern shelf and perhaps enhancing melting. If the flow persists during the summer and/or fall, the warmer water introduced during fall could also delay arrival of ice. Either way, this particular mechanism is probably limited to the region south of M2.

4. Conclusions

The southeastern Bering Sea shelf has warmed markedly over the last decade. In addition, sea-ice

concentration, duration and maximum extent have decreased. Whether these trends continue is clearly dependent upon the large-scale weather patterns, particularly the origin, magnitude and direction of the winds during winter and also the timing of the spring and fall transitions. While warmer ocean temperatures can delay the arrival of ice, if strong arctic winds persist over the shelf for a sufficiently long time, sea ice can and will be advected over M2.

A distant factor that also must be considered is the decrease of ice concentration in the Arctic. Since ice formation in the Bering requires strong, cold winds out of the north, the lack of ice in Arctic Ocean will impact the air temperature and thus the magnitude of the heat flux between the Bering Sea and the atmosphere. It seems reasonable that the western Arctic must freeze before the Bering Sea can freeze. The amount of ice in the Arctic during summer has decreased over the last decade, and there are predictions that it will continue to do so for the foreseeable future (Stroeve et al., 2005). If these predictions prove true, ice concentrations in the Bering also should decrease.

While the Bering Sea shelf has warmed over the last decade, the mechanisms that control this change in temperature are difficult to quantify. Syntheses using the data presented here will provide the foundation for a knowledgeable forecast of how future changes in climate will impact this ecosystem, its living marine resources and protected marine

species. Changes in the physical environment can and will trigger changes in the Bering Sea ecosystem.

Acknowledgments

While NOAA has provided support each year additional funding has been provided by Coastal Ocean Program's Bering Sea FOCI (1995), Southeast Bering Sea Carrying Capacity (SEBSCC: 1996–2001), the International Arctic Research Center and the Cooperative Institute for Arctic Research (IARC: 1999–2001), the Pollock Conservancy (2002) and North Pacific Research Board (2002–2005). Without this critical support the moorings could not have been maintained. We particularly thank the officers and crew of the NOAA ship *Miller Freeman*, W. Parker, W. Floering, C. Dewitt for deploying and recovering the moorings, and D. Kachel and D. Pashinski for processing the data. The comments from two anonymous reviewers were extremely helpful. This publication is partially funded by the Joint Institute for the Study of the Atmosphere and Ocean (JISAO) under NOAA Cooperative Agreement No. NA17RJ1232, Contribution # 1235. "This paper was first presented in the GLOBEC-ESSAS Symposium on "Effects of climate variability on sub-arctic marine ecosystems", hosted by PICES in Victoria, BC, May 2005".

References

- Boldt, J., 2004. Ecosystem Considerations for 2005, Appendix C, Groundfish Stock Assessment and Fisheries Evaluation Report. North Pacific Fishery Management Council, Anchorage, 260pp.
- Bond, N.A., Adams, J.M., 2002. Atmospheric forcing of the southeast Bering Sea Shelf during 1995–99 in the context of a 40-year historical record. *Deep-Sea Research II* 49 (26), 5869–5887.
- Bond, N.A., Overland, J.E., Spillane, M.C., Stabeno, P.J., 2003. Recent shifts in the state of the North Pacific. *Geophysical Research Letters* 30 (23), 2183.
- Brodeur, R.D., Mills, C.E., Overland, J.E., Walters, G.E., Schumacher, J.D., 1999. Evidence for a substantial increase in gelatinous zooplankton in the Bering Sea, with possible links to climate change. *Fisheries Oceanography* 8 (4), 296–306.
- Grebmeier, J.M., Overland, J.E., Moore, S.E., Farley, E.V., Carmack, E.C., Cooper, L.W., Frey, K.E., Helle, J.H., McLaughlin, F.A., McNutt, S.L., 2006. A major ecosystem shift in the Northern Bering Sea. *Science* 311 (5766), 1461–1464.
- Hare, S.R., Mantua, N.J., 2000. Empirical evidence for North Pacific regime shifts in 1977 and 1989. *Progress in Oceanography* 47, 103–145.
- Hunt Jr., G.L., Stabeno, P.J., 2002. Climate change and the control of energy flow in the southeastern Bering Sea. *Progress in Oceanography* 55 (1–2), 5–22.
- Hunt Jr., G.L., Stabeno, P.J., Walters, G., Sinclair, E., Brodeur, R.D., Napp, J.M., Bond, N.A., 2002. Climate change and control of the southeastern Bering Sea pelagic ecosystem. *Deep-Sea Research II* 49 (26), 5821–5853.
- Kalnay, E., et al., 1996. The NCEP/NCAR 40-year reanalysis project. *Bulletin of the American Meteorological Society* 77, 437–471.
- Kowalik, Z., Stabeno, P.J., 1999. Trapped motion around the Pribilof Islands in the Bering Sea. *Journal of Geophysical Research* 104 (C11), 25,667–25,684.
- Ladd, C., Bond, N.A., 2002. Evaluation of the NCEP–NCAR reanalysis in the northeast Pacific and the Bering Sea. *Journal of Geophysical Research* 107 (C10), 3158.
- McKinnell, S., 2004. *The Precautionary Approach to the PDO*, vol. 12(1). PICES Press, pp. 16–17.
- Moore, S.E., Grebmeier, J.M., Davis, J.R., 2003. Gray whale distribution relative to forage habitat in the northern Bering Sea: current conditions and retrospective summary. *Canadian Journal of Zoology* 81, 734–742.
- Napp, J.M., Kendall Jr., A.W., Schumacher, J.D., 2000. A synthesis of biological and physical processes affecting the feeding environment of larval walleye pollock (*Theragra chalcogramma*) in the eastern Bering Sea. *Fisheries Oceanography* 9, 147–162.
- Niebauer, H.J., 1988. Effects of El Niño–Southern Oscillation and North Pacific weather patterns on interannual variability in the subarctic Bering Sea. *Journal of Geophysical Research* 93, 5051–5068.
- Nof, D., Im, S.H., 1985. Suction through broad oceanic gaps. *Journal of Physical Oceanography* 15, 1721–1732.
- Overland, J.E., Stabeno, P.J., 2004. Is the climate of the Bering Sea warming and affecting the ecosystem? *EOS Transactions of the American Geophysical Union* 85 (33), 309–316.
- Overland, J.E., Wang, M., 2005a. The Arctic climate paradox: the recent decrease of the Arctic Oscillation. *Geophysical Research Letters* 32 (6), L06701.
- Overland, J.E., Wang, M., 2005b. The third arctic climate pattern: 1930s and early 2000s. *Geophysical Research Letters* 32 (23), L23808.
- Reed, R.K., Stabeno, P.J., 1996. On the climatological mean circulation over the eastern Bering Sea shelf. *Continental Shelf Research* 16 (10), 1297–1305.
- Rodionov, S., Bond, N.A., Overland, J.E., 2007. The Aleutian low, storm tracks and winter climate variability in the Bering Sea. *Progress in Oceanography* this volume.
- Schumacher, J.D., Stabeno, P.J., 1998. Continental shelf of the Bering Sea. In: Robinson, A.R., Brink, K.H. (Eds.), *The Sea*, vol. 11. Wiley, UK, pp. 789–822 (Chapter 27).
- Stabeno, P.J., Hunt Jr., G.L., 2002. Overview of the inner front and Southeast Bering Sea carrying capacity programs. *Deep-Sea Research II* 49 (26), 6157–6168.
- Stabeno, P.J., Overland, J.E., 2001. The Bering Sea shifts toward an earlier spring transition. *EOS Transactions of the American Geophysical Union* 82 (29), 317–321.
- Stabeno, P.J., Schumacher, J.D., Davis, R.F., Napp, J.M., 1998. Under-ice observations of water column temperature, salinity and spring phytoplankton dynamics: Eastern Bering Sea shelf. *Journal of Marine Research* 56 (1), 239–255.

- Stabeno, P.J., Bond, N.A., Kachel, N.B., Salo, S.A., Schumacher, J.D., 2001. On the temporal variability of the physical environment over the south-eastern Bering Sea. *Fisheries Oceanography* 10 (1), 81–98.
- Stabeno, P.J., Kachel, N.B., Sullivan, M., Whitledge, T.E., 2002a. Variability of physical and chemical characteristics along the 70-m isobath of the southeast Bering Sea. *Deep-Sea Research II* 49 (26), 5931–5943.
- Stabeno, P.J., Reed, R.K., Napp, J.M., 2002b. Transport through Unimak Pass, Alaska. *Deep-Sea Research II* 49 (26), 5919–5930.
- Stroeve, J.C., Serreze, M.C., Fetterer, F., Arbetter, T., Meier, W., Maslanik, J., Knowles, K., 2005. Tracking the Arctic's shrinking ice cover: another extreme September minimum in 2004. *Geophysical Research Letters* 32.
- Wyllie-Echeverria, T., 1995. Sea-ice conditions and the distribution of walleye pollock (*Theragra chalcogramma*) on the Bering and Chukchi Sea shelf. In: Beamish, R.J. (Ed.), *Climate Change and Northern Fish Populations*, vol. 121. Canadian Special Publication of Fisheries and Aquatic Sciences, Canada, pp. 131–136.